Title
Unusual metamagnetism in CeIrIn5

Journal
Physical Review B, 80(9)

ISSN
2469-9950

Authors
Capan, C
Balicas, L
Murphy, TP
et al.

Publication Date
2009-09-01

DOI
10.1103/physrevb.80.094518

Unusual metamagnetism in $CeIrIn_5$

C. Capan,[1,2] L. Balicas,[3] T. P. Murphy,[3] E. C. Palm,[3] R. Movshovich,[4] D. Hall,[3,*] S. W. Tozer,[3] M. F. Hundley,[4] E. D. Bauer,[4] J. D. Thompson,[4] J. L. Sarrao,[4] J. F. DiTusa,[2] R. G. Goodrich,[5,2] and Z.Fisk[1]

[1]*Department of Physics and Astronomy, University of California Irvine, Irvine, CA 92697-4575*

[2]*Department of Physics and Astronomy, Louisiana State University, Baton Rouge, LA 70803*

[3]*National High Magnetic Field Laboratory, Florida State University, Tallahassee, Florida 32310*

[4]*Los Alamos National Laboratory, MST-10, Los Alamos, New Mexico 87545*

[5]*Department of Physics, George Washington University, Washington, DC 20052*

(Dated: November 20, 2013)

Abstract

We report a high field investigation (up to 45 T) of the metamagnetic transition in $CeIrIn_5$ with resistivity and de-Haas-van-Alphen (dHvA) effect measurements in the temperature range 0.03-1 K. As the magnetic field is increased the resistivity increases, reaches a maximum at the metamagnetic critical field, and falls precipitously for fields just above the transition, while the amplitude of all measurable dHvA frequencies are significantly attenuated near the metamagnetic critical field. However, the dHvA frequencies and cyclotron masses are not substantially altered by the transition. In the low field state, the resistivity is observed to increase toward low temperatures in a singular fashion, a behavior that is rapidly suppressed above the transition. Instead, in the high field state, the resistivity monotonically increases with temperature with a dependence that is more singular than the iconic Fermi-liquid, temperature-squared, behavior. Both the damping of the dHvA amplitudes and the increased resistivity near the metamagnetic critical field indicate an increased scattering rate for charge carriers consistent with critical fluctuation scattering in proximity to a phase transition. The dHvA amplitudes do not uniformly recover above the critical field, with some hole-like orbits being entirely suppressed at high fields. These changes, taken as a whole, suggest that the metamagnetic transition in $CeIrIn_5$ is associated with the polarization and localization of the heaviest of quasiparticles on the hole-like Fermi surface.

Itinerant Electron Metamagnetism (IEM) refers to a field induced transition from a paramagnetic (PM) to a field-polarized paramagnetic state, first predicted for exchange-enhanced paramagnets such as Pd[1]. The effect is intriguing since large, almost discontinuous changes in the magnetization can be observed through such a transition. In fact such field-induced magnetization jumps have usually been interpreted as a dramatic change in the density of states (DOS) at the Fermi energy as a Zeeman split DOS peak crosses the Fermi level. The most spectacular examples of IEM have been observed in the $MgCu_2$ type cubic Laves phases such as $A\mathrm{Co}_2$ (A=Sc, Y, Lu)[2]. In heavy fermion systems, the screening of local moments by conduction electrons leads to a Kondo resonance peak in the DOS close to the Fermi level, so that large magnetic fields can lead to IEM behavior. Among the first heavy fermion compounds reported to have a metamagnetic transition are UCoAl[3], and UPt_3[4], and, by far the most thoroughly investigated, $\mathrm{CeRu}_2\mathrm{Si}_2$[5]. Theoretical approaches that take into account the spin fluctuations can successfully capture the basic features of IEM in Laves phase compounds[6]. In order to capture some of the more subtle aspects of IEM in heavy fermion systems, Hubbard or Anderson model physics must be included. These models can reproduce features such as the Fermi surface volume change inferred from the dHvA[7] and due to f-electron localization[8], as well as the sign change of the exchange coupling[9] (from antiferro- to ferromagnetic) observed in neutron scattering[10].

Despite a great amount of both theoretical and experimental work, some of the essential questions about IEM remain unsolved. For instance, is there a common picture emerging between the d- and f-electron systems that exhibit IEM? Would it involve solely a change in Fermi surface geometry (along with a magnetoelastic instability) or include a change in the volume enclosed by the Fermi surface? This is a particularly relevant issue for the heavy fermion systems, since Fermi surface changes have been observed under applied field[11,12] and pressure[13] and it is not clear if this indicates f-electron localization due to field polarization of the conducting electrons. Finally the discovery of IEM in the Ruddlesden-Popper compounds $\mathrm{Sr}_3\mathrm{Ru}_2\mathrm{O}_7$ and $\mathrm{Sr}_4\mathrm{Ru}_3\mathrm{O}_{10}$ has opened new horizons[14–16]. Systematic deviations from the Fermi Liquid (FL) theory are reported in the resistivity (ρ)[15], thermal expansion[17], and NMR[18] near the metamagnetic transition in $\mathrm{Sr}_3\mathrm{Ru}_2\mathrm{O}_7$, raising the possibility of a field-induced quantum critical point (QCP) in IEM systems. The $T = 0$ suppression of a first order metamagnetic discontinuity terminating at a critical end-point has been shown theoretically to result in a QCP[19], a situation potentially realized in $\mathrm{Sr}_3\mathrm{Ru}_2\mathrm{O}_7$. The role of

disorder[20,21] as well as the formation of magnetic domains[22] in the proximity of a metamagnetic transition are still under investigation.

Here we report a high field investigation of the recently discovered IEM transition in $CeIrIn_5$[23–25], to search for evidence of a metamagnetic QCP. $CeIrIn_5$ is a heavy fermion superconducting member of the layered tetragonal $CeMIn_5$ (M=Rh,Ir,Co) family[26]. Since their discovery, the 1-1-5 compounds have been the focus of much attention because they exhibit striking deviations from FL theory. There has been a great deal of work trying to understand the origin of such anomalous behavior in strongly correlated systems[27] and descriptions are often based on the proximity to a QCP in their phase diagrams. Near such a singular point where a magnetic phase transition is driven to $T = 0$ by an external tuning parameter (pressure, magnetic field or doping) the presence of quantum fluctuations is expected to have a strong effect on all physical properties, leading to the breakdown of the FL theory. In particular, the 1-1-5 compounds have rich and complex phase diagrams, with notably a field tuned QCP near the superconducting upper critical field in $CeCoIn_5$[28–30] and a pressure tuned QCP in $CeRhIn_5$[13,31]. Besides their phase diagram, their heavy fermion state has also attracted attention in its own right. A careful analysis of the transport and thermodynamic properties of La-diluted $CeCoIn_5$ and $CeIrIn_5$ suggests that the coherent heavy fermion ground state coexists with a finite fraction of single-ion Kondo centers down to the lowest T[32]. This conclusion was further supported by optical conductivity measurements on $CeMIn_5$ samples that revealed a broad hybridization between the conduction electrons and the more localized f-electrons which included contributions from 4 electronic bands[33]. In addition, the hybridization gaps that result appear to have extensive momentum dependence with regions where the smallest gap, associated with a particular hole band (β orbits in de Haas-van Alphen experiments), is seen to go to zero. The conclusion was that Kondo screening could be incomplete, particularly in regions where the hybridization gap goes to zero. Band structure calculations using DMFT, motivated by the optical conductivity measurements, have found two distinct hybridization gaps in $CeIrIn_5$, attributed to two distinct In sub-bands hybridizing with the Ce lattice[34].

In addition to the many common trends with its Co and Rh counterparts, a distinguishing feature of $CeIrIn_5$ is the presence of a metamagnetic-like transition near 30 T for the [001] field orientation (perpendicular to the $CeIn_3$ planes). This transition is characterized by a non-linear increase in magnetization[23,24] and a λ-like anomaly in the specific heat[25].

Because the family of 1-1-5 compounds has many unusual features, including what appear to be unusual transitions perhaps associated with interesting QCPs, we are compelled to explore the possible existence of a metamagnetic QCP in $CeIrIn_5$. Our earlier specific heat and ρ measurements up to 17 T have shown a field-induced non-Fermi Liquid behavior (NFL). However the limited field range of these experiments did not allow us to explore the immediate vicinity of the metamagnetic transition[35]. We have subsequently extended our investigations to higher fields (up to 45 T) and explored the angle dependence of the high field transition in $CeIrIn_5$ combining resistivity and torque magnetometry measurements[36]. Here, we give a complete account of our high field investigations with an in-depth analysis in search for Fermi surface changes at the transition and for clues about the cause of the NFL behavior.

Our measurements reveal several changes that occur at or near the metamagnetic critical field which have important consequences for interpreting the mechanism for IEM in $CeIrIn_5$. The most obvious is that an increased scattering rate for charge carriers results in an increased resistivity and a decreased dHvA amplitude in the region of the transition. This is accompanied by a resistivity anomaly at very low temperature that switches from increasing resistivity with decreasing temperature below the transition, to decreasing resistivity with decreasing temperature above the transition, none of which can be interpreted as a Fermi liquid-like behavior. Finally, we observe the complete suppression of two of the heaviest dHvA orbits in the high field state, while other orbits recover and eventually exceed their lower field amplitude. These changes are *not* accompanied by significant variations in either the dHvA frequency, indicating no measurable change to the extremal areas of the Fermi surface, or the cyclotron masses associated with orbits that we observe. Our data indicate that light parts of the Fermi surface are left unchanged by the IEM while the heavier parts are suppressed beyond the metamagnetic critical field. Although our data do not provide direct evidence for a metamagnetic QCP, we observe NFL transport properties in proximity to the critical field as well as an instability of the heaviest Fermi surface sheet, both of which are consistent with quantum critical behavior.

The paper is organized as follows: we first present the high field phase diagram of $CeIrIn_5$, which has been previously established via magnetization[23] and specific heat measurements[25]. This is followed in section III by a description of the resistivity anomalies associated with the metamagnetic transition. Section IV is devoted to the evolution of the Fermi surface

across the metamagnetic transition, with an analysis of the dHvA oscillations observed in the torque signal. Finally, in section V we summarize the conclusions that our data make necessary.

I. EXPERIMENTAL DETAILS

Isothermal magnetoresistance sweeps have been performed using standard four probe techniques and a low frequency resistance bridge, on two single crystals at the National High Magnetic Field Laboratory, using the 33 T resistive magnet for the first and the 45 T hybrid magnet for the second sample. The samples were pre-screened for In inclusions (by checking for superconducting signal in the resistivity at the T_c of In) and mounted on a rotating sample holder inside the mixing chamber of a top loading dilution refrigerator. The sample $S1$ was measured with a current of 300 μA up to 33 T at a fixed angle of 14^o with respect to [001]. These data were later complemented by measurements up to 45 T on sample $S2$ with varying angle and a current of 1 mA. For both samples, the current is applied perpendicular to [001]. The field was rotated from [001] to a direction parallel to the ab-plane, but perpendicular to the applied current. The samples were allowed to thermalize for about 1 hr and the temperature of the mixing chamber was recorded at 0 T ($S1$) and 12 T ($S2$) before each field sweep. Simultaneous torque magnetization measurements have been performed using an AC capacitance bridge on a sample cut from the first crystal ($S1$) and mounted with G.E. varnish on a Cu-Be cantilever.

II. PHASE DIAGRAM

The high field phase diagram has been previously established by magnetization[23] and specific heat[25] measurements. Figures 1a and 1c show the derivative of the torque signal as a function of magnetic field, H, for temperatures ranging between 0.04 and 0.92 K at fixed angle (-8°) and, in Fig. 1c, for angles (Θ) between H and [001] ranging from -1° to 29° at our base temperature (0.04 K). The torque signal is proportional to the vector product of magnetization with magnetic field and is shown for $\Theta = -8^o$ and $T = 0.04$ K as an inset (see Fig. 1b). The torque signal is reported in Fig. 1 in arbitrary units since the cantilever used was uncalibrated. The feature in the torque signal, indicated by an arrow in figure 1b , or

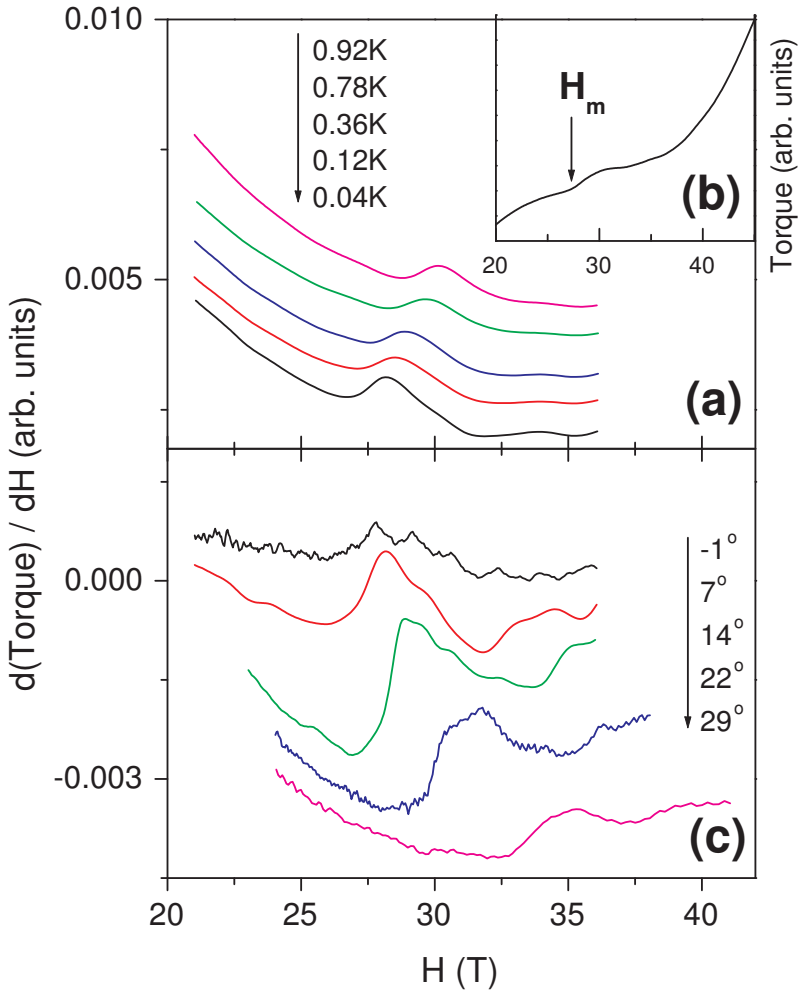

FIG. 1: Torque signal near the metamagnetic critical field. (a) Derivative of Torque signal vs. applied magnetic field, H, in $CeIrIn_5$ in the field range 20-35 T at an angle of $-8°$ for temperatures ranging between 0.04 and 0.92 K. The peak corresponds to the metamagnetic transition. (b) Torque signal at 0.04 K (in arbitrary units) vs. H between 20 and 45 T for $\Theta = -8°$. The metamagnetic field H_m is indicated by an arrow. (c) Derivative of the Torque signal vs. H for field orientations ranging between $-1°$ and $29°$ at the base temperature of 0.04 K. The data are shifted vertically for clarity.

equivalently the peak in the derivative, Fig. 1a and 1c, marks the metamagnetic transition field H_m. H_m is seen to shift to higher fields with increasing temperatures and angles. On the $H-T$ phase diagram, shown in Fig. 2, the transition determined from torque data (at $\Theta = -8°$ from [001]) extends to lower temperatures the previously reported transition line determined from the specific heat[25]. The transition field H_m increases nearly quadratically

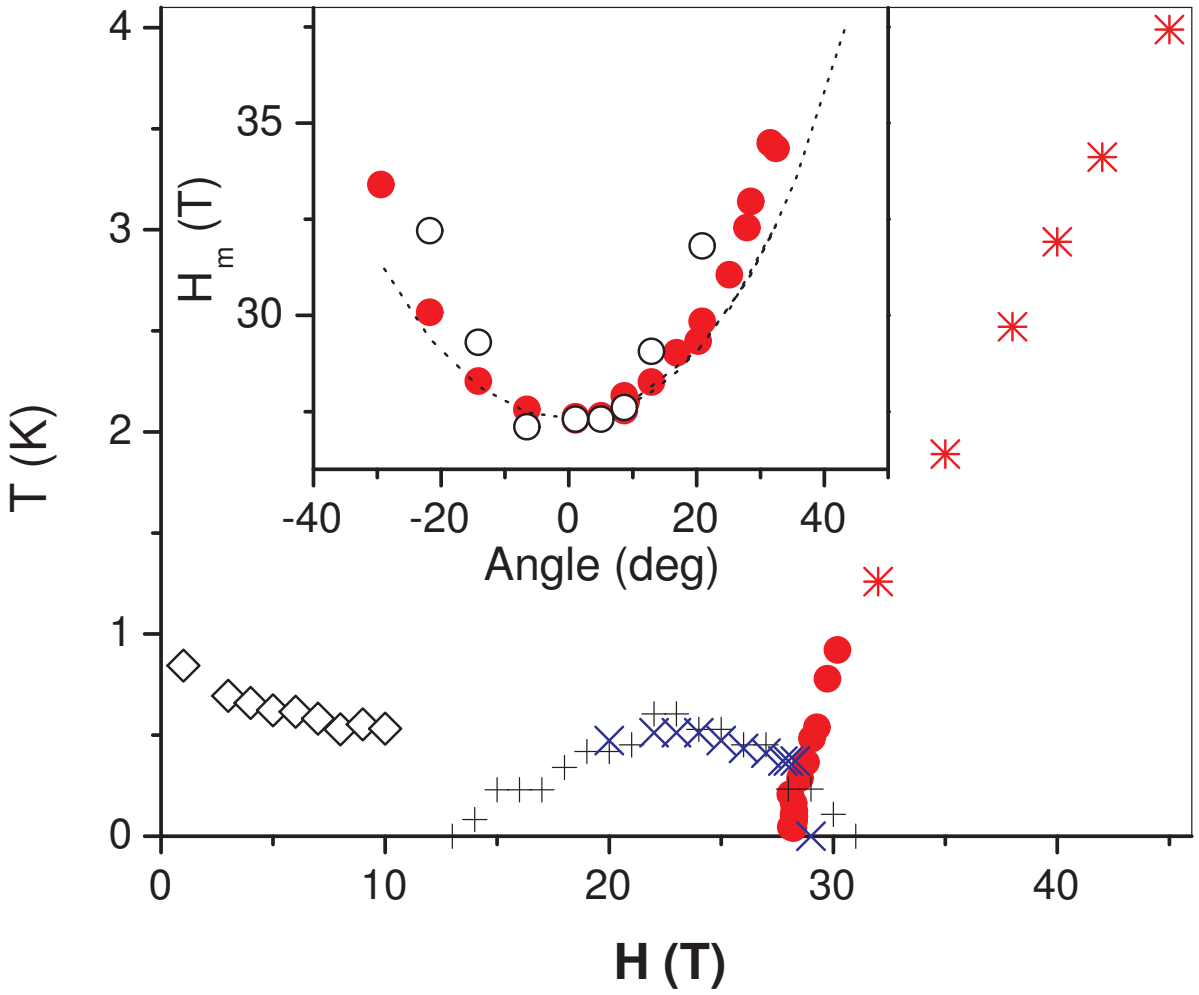

FIG. 2: Magnetic field phase diagram in $CeIrIn_5$ for $H\|[001]$. The metamagnetic transition H_m is determined from torque magnetometry ($\bullet$) and from specific heat data of Ref.[25] ($*$). The Fermi Liquid crossover temperature is determined from our previous specific heat data[35] ($\diamond$). The resistivity minimum for the two samples $S1$ ($\times$) and $S2$ ($+$) are also shown. Inset: Angular dependence of the metamagnetic field H_m determined from magnetization ($\bullet$) and from resistivity ($\circ$) at 0.04 K. The angle (Θ) is defined between the magnetic field and [001]. The dashed line correspond to a fit to $H_m = H_m(0)\frac{1}{cos(\Theta)}$.

in temperature. This dependence of $H_m(T)$ is also observed in the Laves compounds and is consistent with Ginzburg-Landau theory[6]. The angular dependence of H_m, shown in the inset of Fig. 2, can be fit to a $\frac{1}{cos(\Theta)}$ dependence, suggesting that only the component of the field parallel to [001] induces the transition. In fact no transition is observed up to 60 T for fields along the ab-plane[23]. The transition is most likely second order in the phase

space of temperature, field and angle that we explored, with no sharpening of magnetization anomaly into a first-order like discontinuity upon cooling, in contrast to the previous claim of Ref.[25]. Although we cannot exclude a weakly first order transition, the torque data do not show any evidence for a critical end-point in $CeIrIn_5$, as is the case for $Sr_3Ru_2O_7$[15]. The transition can be extrapolated to $T = 0$ around $H_m(T = 0) = 28$ T. Thus the phase diagram suggests the possibility of a metamagnetic QCP for $H \parallel [001]$. Also shown in the phase diagram is the crossover line from Fermi Liquid to non-Fermi Liquid regime obtained in our earlier specific heat (C) investigation (up to 17 T) as the temperature below which $\frac{C}{T}$ becomes constant.

III. MAGNETORESISTANCE

The transition observed in $M(H)$ is also apparent in the resistivity data shown in Fig. 3. The magnetoresistance (MR) in $CeIrIn_5$ is positive at low T, except around H_m. Indeed, ρ goes through a broad maximum and decreases above H_m for fields oriented close to [001] ($\Theta \leq 12^o$) (Fig. 3b). With a further increase of H, ρ increases steeply in the high field state. The field at which ρ is maximum closely follows the same temperature and angular dependence as H_m determined from magnetization, and is also shown in the inset of Fig. 2. Note that a crossover from positive to negative MR has been reported in the related compound $CeCoIn_5$[28], however, its relation to a possible metamagnetic transition is not well established. With increasing Θ the peak shifts to higher fields and becomes less pronounced: at $\Theta = 20^\circ$ a plateau is observed. A small change in the slope can still be resolved at $\Theta = 27^\circ$ but no hint of a transition is observed at $\Theta = 34.5^\circ$.

The temperature dependence of the resistivity is constructed from the isothermal sweeps, Fig. 3, and is shown for a range of fields in Fig. 4 where ρ is plotted as a function of T^2. The resistivity is consistent with a T^2 dependence between 0.04 K and 0.92 K at fields larger than 36 T where the sample has entered the field-polarized paramagnetic state. This is as expected for the case of a Fermi liquid ground state. Fits to a T^2 dependence to our data are shown as solid lines in Fig. 4a for fields between 37 and 45 T. The slope in $\rho = \rho_0 + A_{FL}T^2$ defines the Fermi Liquid coefficient A_{FL}, with $A_{FL} \sim 0.972$ $\mu\Omega$ cm/K^2 (at $H = 45$ T) corresponding to a specific heat coefficient of $\gamma \sim 0.54$ J/K^2 mol (using the Kadowaki-Woods ratio obtained for $CeCoIn_5$ in Ref.[29]), which is close to the experimental

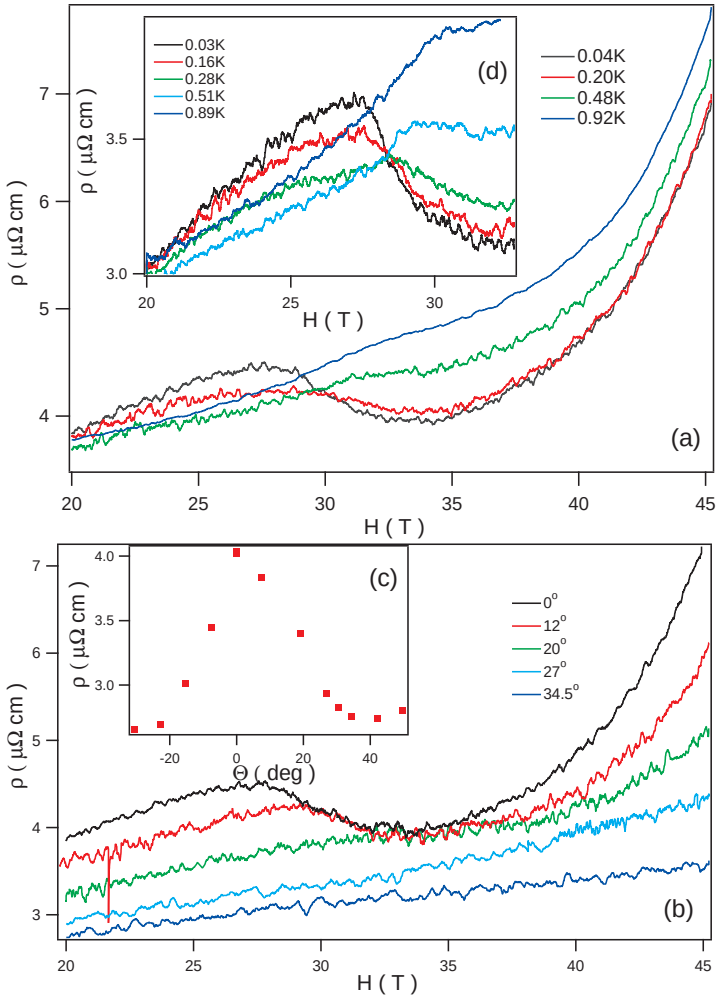

FIG. 3: Magnetoresistance in $CeIrIn_5$. Resistivity ρ vs applied magnetic field H in $CeIrIn_5$ for the sample $S2$ measured up to 45 T (a) for indicated temperatures at $\Theta = -8^o$ (b) for various angles Θ between the field and the [001] orientation at the base temperature of 40 mK. Insets: (c) Angular dependence of ρ at $T = 40$ mK and $H = 20$ T in sample $S2$. (d) Resistivity vs applied magnetic field for the sample $S1$, measured up to 33 T, for indicated temperatures, at fixed angle $\Theta = 14^o$.

value found in $CeIrIn_5$ at $H = 45$ T ($\gamma \sim 0.4$ J/K^2 mol in Ref.[25]), and slightly suppressed compared to $\gamma \sim 0.75$ J/K^2 mol at $H = 1$ T[35], as expected. This estimate suggests that the field-polarized state is still a heavy fermion metal, a conclusion also supported by the analysis of the cyclotron effective masses (see below).

In contrast, for fields just above H_m there is a strong deviation from a T^2 dependence of ρ at the lowest temperatures. Here the resistivity has a temperature dependence weaker than quadratic, as evidenced by the downward curvature in the figure for sample $S2$ (Fig. 4b) be-

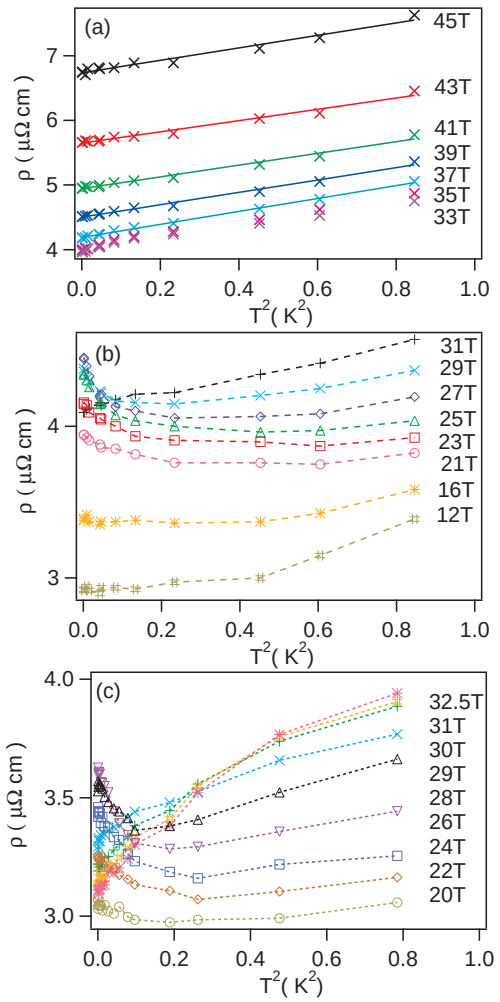

FIG. 4: Temperature dependence of resistivity in $CeIrIn_5$ for a field applied at $\Theta = -8^o$ from [001]. Resistivity, ρ, vs temperature, T, squared (a),(b) for the sample $S2$ between 12 and 45 T in the T-range $0.04 - 0.92$ K and (c) for the sample $S1$ between 20 and 32.5 T in the T-range $0.03 - 0.87$ K. Solid lines in (a) are linear fits to ρ vs. T^2.

tween 33 and 35 T, and for sample $S1$ between 30 and 32.5 T (Fig. 4c). This non quadratic T-dependence of ρ occurs very close to the critical field, H_m, for both $S1$ and $S2$. In a previous publication, where we measured a different $CeIrIn_5$ sample, we found that ρ was not well described by a Fermi liquid-like T^2 dependence for temperatures down to 50 mK and magnetic fields of 12, 15, and 17 T oriented parallel to the [001] direction whereas a T^2 dependence was found with the field oriented perpendicular to [001][35]. This stresses the importance of magnetoresistance effects in the high field regime for the $T-$dependence of ρ, which can make the interpretation of non-Fermi Liquid behavior problematic. However, the

anomalous temperature dependence of ρ in $CeIrIn_5$ is clearly associated with the metamagnetic transition since the quadratic-in-T behavior is recovered for fields well above H_m. Note that the occurrence of non Fermi-liquid like behavior in the resistivity is somewhat at odds with the simultaneous observation of quantum oscillations. This suggests that the inelastic (electron-electron) scattering responsible for the former becomes negligible compared to the elastic (disorder) scattering at very low T. This situation is *not* unique to $CeIrIn_5$: $CeCoIn_5$ also exhibits non-Fermi Liquid behavior concomitant to quantum oscillations close to its superconducting upper critical field[28–30,37]. Our observation of a non-quadratic temperature dependence of ρ near H_m is in direct conflict with the observation of a resistivity well described by a T^2 dependence across the metamagnetic transition in $CeRu_2Si_2$[39], suggesting a separate mechanism for IEM in these two heavy fermion systems.

For fields below H_m, a new contribution to ρ appears with a negative $d\rho/dT$ below $\sim$ 0.5 K, as seen in Fig. 4. This low-T upturn in ρ becomes more pronounced in the vicinity of the metamagnetic field, and is rapidly suppressed above it. The temperature $T_{\rm min}$ where $\rho(T)$ has a minimum is field dependent and defines the dome-shaped region in the $H-T$ phase diagram, as shown in Fig. 2. We note that there is no anomaly associated with $T_{\rm min}$ in the torque signal. This behavior has been observed in two different crystals at two different field orientations close to [001], and so it is a robust and reproducible feature of the metamagnetic transition in $CeIrIn_5$.

An upturn in ρ in the presence of high magnetic field is also observed at low$-T$ in $CeCoIn_5$[28,30] and UPt_3[40]. This contribution becomes more pronounced as the field is increased. It has been so far associated with the cyclotron magnetoresistance in the high field limit ($\omega_c\tau \sim 1$), since it is only observed in the transverse geometry. An upturn is indeed possible in the high field limit of a compensated metal with $\rho(H,T) \sim \frac{H^2}{(\rho_0+AT^2)^2}$. The upturn in $CeIrIn_5$ is saturating at low T and can be reasonably well described by this form. However, its suppression above the metamagnetic field is at odds with this scenario. This cannot be accounted for by the negative contribution to MR compensating the positive one, since MR is only negative close to H_m and the upturn in ρ is *not* recovered when the MR becomes positive above 36 T. Moreover, the dome-shaped onset temperature $T_{\rm min}$, as shown in Fig. 2, clearly does not track the crossover to the high field regime ($\omega_c\tau \sim 1$), in striking contrast to $CeCoIn_5$[28,30]. To summarize, although MR effects in the high field

regime may account for the upturn in $\rho(T)$, the suppression of this feature in the field polarized state, in the absence of Fermi Surface change(see below), suggests that a different mechanism is involved in $CeIrIn_5$.

In $Sr_3Ru_2O_7$, a similar, but more pronounced, resistivity anomaly has been observed in the cleanest samples[20] and has been tentatively assigned to the condensation of a nematic phase surrounding the QCP[21]. This is considered as a strong possibility in $Sr_3Ru_2O_7$ since there are first order-like boundaries within which the resistivity anomaly occurs, making the idea of a phase transition appealing. The most likely candidate for such a domain-wall scattering scenario is Condon-like domains[22], and the first order nature of the transitions makes the inhomogeneous state hypothesis a sensible one. Despite similar residual resistivities, the transition at H_m in $CeIrIn_5$ is not as sharp as the one observed in $Sr_3Ru_2O_7$. Although we cannot rule out the possibility of a common mechanism, the absence of a sharp first order boundary make the domain wall scenario unlikely in $CeIrIn_5$.

An alternative explanation for the low-T resistivity anomaly near H_m in $CeIrIn_5$ relies on the scattering of quasiparticles from quantum magnetic fluctuations leading to a crossover into a diffusive transport regime. This idea is consistent with the prediction that any deviation from Fermi Liquid behavior in presence of disorder will lead to an infinite resistivity at $T = 0$[41]. Moreover, logarithmic corrections to the conductivity, due to enhanced impurity scattering in the presence of strong quantum fluctuations, have been predicted for a ferromagnetic[42,43], and more recently for a metamagnetic[44], quantum critical point. The idea is that near the QCP, the diverging magnetic coherence length (with decreasing T) eventually becomes larger than the mean free path (ℓ) (or equivalently, the correlation time becomes larger than the time between successive collisions) and the system effectively behaves as if it were impurity scattering limited. This is similar to what was previously reported in the itinerant ferromagnet $Fe_{1-x}Co_xSi$[45]. The crossover from ballistic to disordered regime is expected to occur near $T_0 = \frac{\hbar\tau^{-1}}{k_B} \sim 0.62$ K in $CeIrIn_5$ which is of the order of $T_{\min}$. Here we have used the Drude model along with the measured linear temperature coefficient of the specific heat ($\gamma_0 = 0.75$ J mol^{-1} K^{-2} defined at $H = 1$ T), along with estimate of the electron density, 2.9 electron per Ce ion based on the Hall coefficient at 300 K[46], $n = 17.98 \times 10^{27}$

m^{-3}, in order to estimate the scattering time :

$$\tau = \frac{m^*}{ne^2\rho} = \frac{\gamma_0}{(\frac{\pi}{3})^{2/3}(\frac{k_B}{\hbar})^2 n^{4/3} e^2 \rho}, \tag{1}$$

with the result that $\tau \sim 1.2\ 10^{-11}$s. However, as we lack convincing evidence of a QCP at H_m in $CeIrIn_5$, this hypothesis must be viewed as only a possibility.

In summary, we believe several of the suggested mechanisms for the origin of the MR can be effectively ruled out, and one of them, quantum corrections in a diffusive transport regime, depends heavily on the existence of a QCP at H_m, which we do not have conclusive evidence for at this time. In addition, the presence of non-quadractic $T-$dependence in ρ, which is clearly related with the metamagnetic transition in $CeIrIn_5$, distinguishes it from the prototypical heavy fermion metamagnet $CeRu_2Si_2$. We note that in the latter, a metamagnetic QCP has been recently ruled out based on lower temperature, higher precision, resistivity measurements[39]. The low$-T$ upturn as well as the non-quadratic behavior in ρ raise important questions and present a challenge for understanding the unusual behavior that we observe in $CeIrIn_5$.

IV. DE-HAAS-VAN-ALPHEN EFFECT

The study of the Fermi surface in heavy fermion metals via quantum oscillations of magnetization (dHvA effect) was pioneered by Taillefer et. al[48]. These oscillations result from the discontinuity in the Fermi-Dirac distribution at $T = 0$ and are well understood in simple metals in the framework of Lifshitz-Kosevich (LK) theory[49]. The observation of dHvA oscillations in heavy fermion metals is an important experimental milestone showing that these strongly correlated compounds can simply be described in terms of heavy quasi-particles, Landau quasiparticles with cyclotron masses much larger than band masses. The Onsager relation dictates that the dHvA frequencies are proportional to the cross-sectional area(s) of the Fermi surface perpendicular to the applied field. Therefore, by mapping the angular dependence of the frequency one can determine the Fermi Surface topography. This has been done in the 1-1-5 compounds, with the observed quasi-2D α (electron) and β (hole) FS sheets in close agreement with band structure calculations[37,50,51]. These results indicate that both $CeCoIn_5$ and $CeIrIn_5$ have itinerant f-electrons at low temperatures,

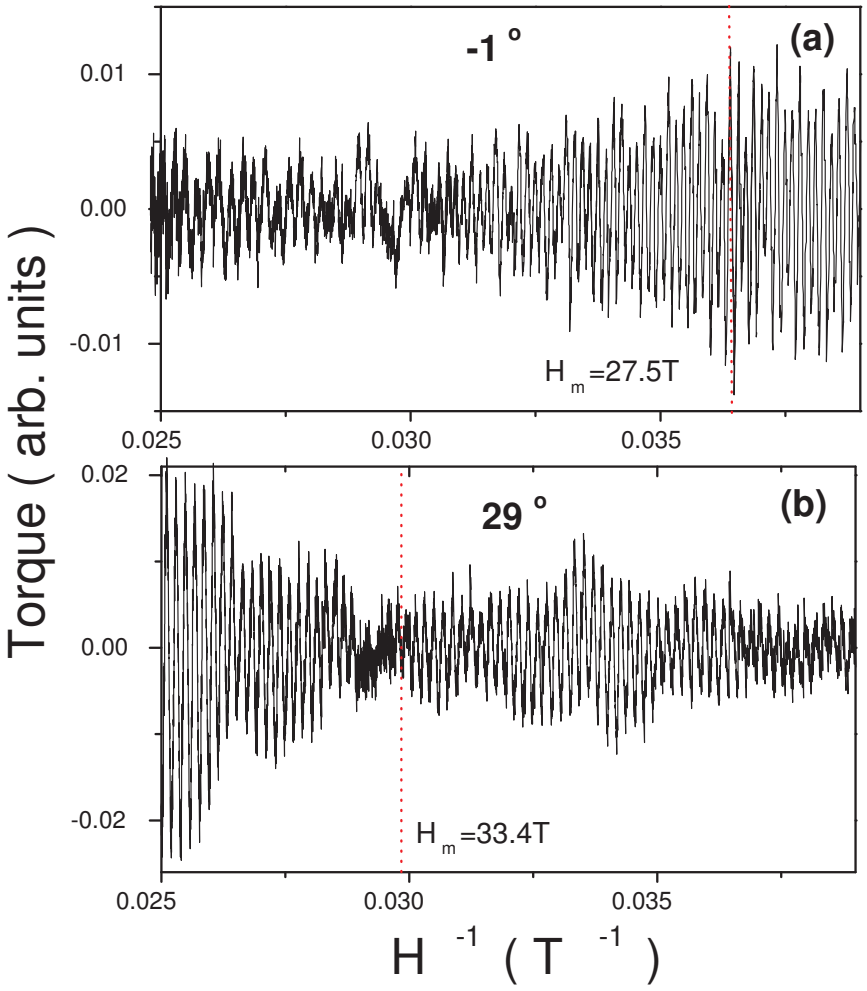

FIG. 5: De Haas-van Alphen oscillations in $CeIrIn_5$. Torque signal (after subtraction of a smooth background) vs inverse magnetic field H^{-1} at $\Theta = -1°$ (a) and 29° (b). The corresponding field range is 25.6 to 40 T. The dashed line indicates the metamagnetic transition field H_m =27.5 T and 33.4 T for the two angles.

whereas $CeRhIn_5$ has localized f-electrons. Moreover, a band-by-band investigation of the mass enhancement is possible with the dHvA technique, complementing the Fermi surface averaged effective mass given by the specific heat coefficient. By determining the angular dependence of the cyclotron mass it has been possible to identify "hot spots" in the parent cubic compound $CeIn_3$[52].

Figure 5 shows the torque signal in $CeIrIn_5$ (in arbitrary units) as a function of inverse magnetic field H^{-1}, in the field range 25.6-40 T, at the base temperature 0.04 K, for two

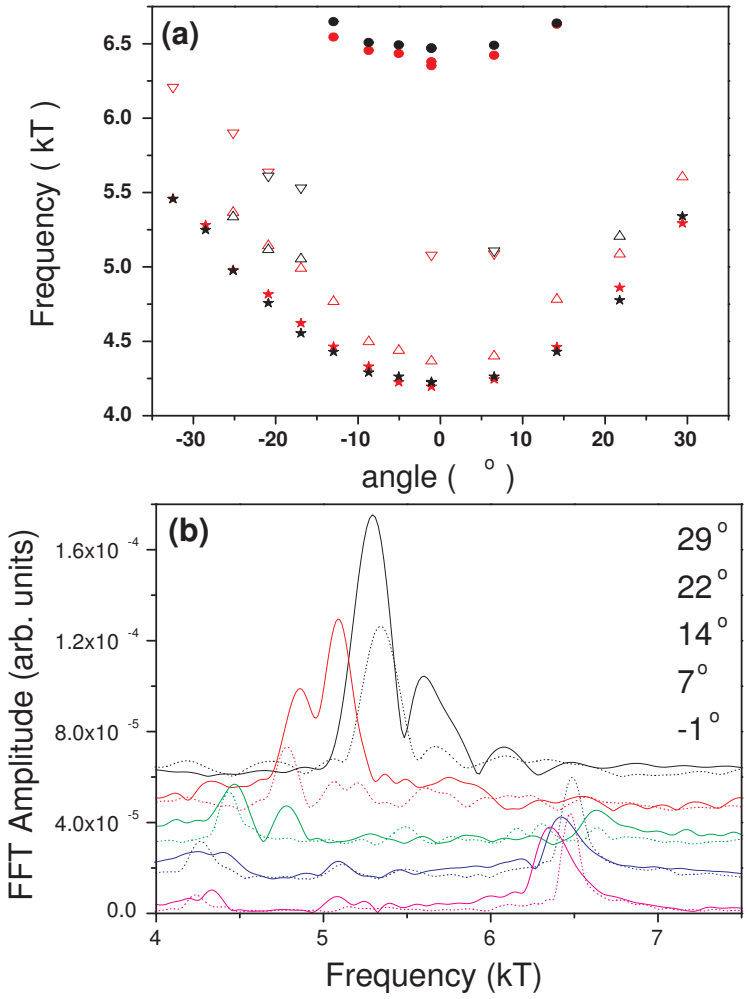

FIG. 6: Angle dependence of the de Haas-van Alphen frequencies in $CeIrIn_5$. (a) Frequency vs Angle in the low field (black symbols, $H < H_m$) and high field states (red symbols, $H > H_m$) corresponding to dHvA branches α_1 ($\triangle$), α_2 ($\triangledown$), α_3 ($\star$) and β_2 ($\bullet$). Zero angle corresponds to $H \parallel [001]$. The β_1 orbit (at 10.4 kT) is only observed for $\Theta = 14°$ and is not shown in this figure. (b) Fast Fourier Transform (FFT) spectra of the torque signal vs frequency in the low field (dashed lines) and high field (solid lines) states for field oriented at 29°, 22°, 14°, 7° and -1° from [001] (top to bottom).

extreme angles $-1°$ and 29°. The background field dependence (shown in Fig. 1b) was determined from a 5^{th} order polynomial fit to the torque signal and then subtracted from the data to better reveal the oscillations in the torque signal which are periodic in H^{-1} corresponding to the dHvA effect. The dHvA frequencies are determined from the Fast Fourier Transform (FFT) spectra of the torque signal at each angle, shown in Fig. 6b. The

FFT is performed on two field intervals of equal length in H^{-1} for $H < H_m$ and $H > H_m$, thus keeping the same frequency resolution to allow comparison. Fig. 6a compares these dHvA frequencies below and above the metamagnetic transition on an angular interval of $\pm 30^\circ$ around [001]. The observed frequencies correspond to extreme orbits on the α and β sheets of the Fermi surface, in agreement with previous reports (up to 16 T) in both their value and their angular dependence. The lower frequencies[50,53], associated with the 3D electron pockets, are not easily detected in torque magnetometry since the torque signal is proportional to the angular derivative of the frequency (see Ref.[49], p.87). Overall, the same branches are observed both below and above H_m, with only a slight shift in frequency across the metamagnetic transition. Moreover, within our frequency resolution (set by the field range of the FFT), we do not see any Zeeman splitting of the α nor β peaks. This is generally the case in metals, as the Zeeman energy is small compared to the Fermi energy[11,12]. These results rule out a major Fermi Surface reconstruction associated with the α and β Fermi surface sheets accompanying the metamagnetic transition in $CeIrIn_5$.

In the LK theory[49], the effective cyclotron mass is determined from the temperature dependence of the amplitude of the dHvA oscillations. The dHvA amplitudes decrease with increasing temperature due to the thermal broadening of the Landau levels crossing the Fermi surface. We have determined the dHvA amplitudes by performing a FFT on intervals of equal length in inverse magnetic field H^{-1} centered around a field value ranging between 20 and 33 T for the first data set ($\Theta = 14^o$) and between 20 and 45 T for the second data set ($\Theta = -8^o$). Each interval contains a fixed number of periods of a given dHvA frequency: 29 periods of α_3 and β_2 at -8° (45 T data set) and 23, 35, and 37 periods of α_3, β_2 and β_1 at 14° (33 T data set). The integer number of periods in a given field interval ensures no artificial broadening of the peaks with the periodic boundary conditions used in the FFT. The temperature dependence of the dHvA amplitudes is then fit to the LK formula in order to determine the effective masses for each branch at a given field (see Ref.[49], p.60):

$$A = A_0 \frac{xT}{sinh(xT)},$$

with $x = \frac{\alpha \frac{m^*}{m_e}}{H}$, where A is the dHvA amplitude, A_0 the $T = 0$ amplitude, m^* the effective mass, m_e the bare electron mass, and $\alpha = \frac{\pi^2 k_B}{\mu_B} = 14.69$ T/K. The data and fits shown in Figs. 7(a) and 7(b) are from FFT spectra on a field range below $H_m(0) = 28$ T. The

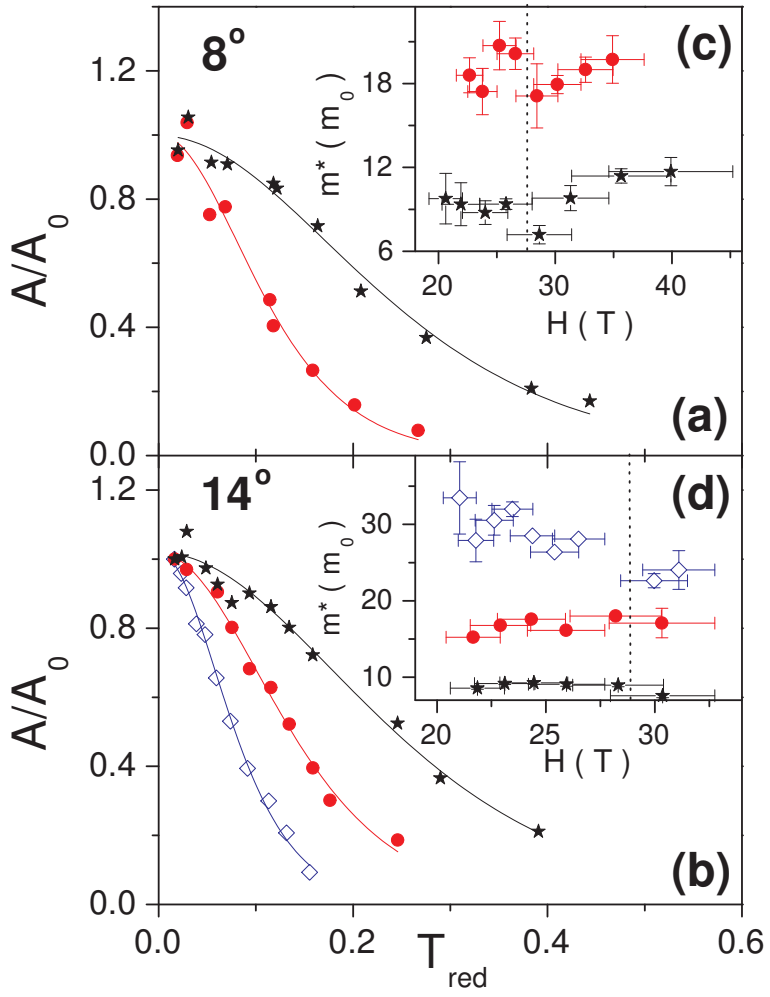

FIG. 7: Determination of effective masses from dHvA in $CeIrIn_5$. (a) and (b) Normalized dHvA Amplitude, A, vs reduced temperature, $T_{red} = \frac{\pi^2 k_B T}{\mu_B H}$, for orientations of $\Theta = -8°$ and $\Theta = 14°$ between H and [001], for the branches $\alpha_3(\star), \beta_2(\bullet), \beta_1(\diamond)$. The amplitudes shown are from the FFT spectra on a small field range below H_m. The solid lines are fits to data with the Lifshitz-Kosevich (LK) formula (see text) with A_0 and m^* being adjustable parameters. The amplitudes shown are normalized with respect to A_0, the $T = 0$ value. (c) and (d) Effective mass vs magnetic field for $\Theta = -8°$ and $\Theta = 14°$ determined from the LK fits. The dashed lines correspond to the IEM transition field H_m. The vertical and horizontal error bars represent the uncertainty in the fitting parameter and the field range of the FFT respectively. The FFT is performed on intervals of equal length in H^{-1} centered around the indicated fields, corresponding to 29 periods for each branch for the 45 T data (a) and 23, 35 and 37 periods for α_3, β_2 and β_1 for the 33T data (b).

field evolution of m^* across the metamagnetic transition is determined in this fashion for each dHvA branch and is shown in Figs. 7(c) and 7(d). The cyclotron mass decreases with increasing field for the β_1 orbit, and is rather field independent for the other two orbits, α_3 and β_2. In contrast to other metamagnetic systems[54–56], no divergence of m^* is observed in any branch for fields near H_m, within the finite field resolution of our procedure set by the field interval of the FFTs. For the branches α_3 and β_2 the effective masses show no significant angular variation between $\Theta = -8^\circ$ (Fig. 7(c)) and $\Theta = 14^\circ$ (Fig. 7(d)). At -8^o, the β_1 orbit is not resolved, possibly due to its large mass. The effective masses we obtained are also in close agreement with the previously reported masses for magnetic fields below 16 T in the [001] direction[51].

The evolution of the Fermi surface has been studied via dHvA effect in a number of heavy fermion compounds across metamagnetic transitions[12,54,55,57]. These studies have shown that the IEM is in general accompanied by drastic changes both in the effective mass and in the dHvA frequencies. This frequency change has been ascribed to f-electron localization in $CeRu_2Si_2$[54,55] or to Zeeman splitting (Fermi surface polarization) in UPt_3[57]. In the light of these results, the absence of a substantial frequency change in $CeIrIn_5$ is striking, despite the fact that the field scale of H_m is comparable to or larger than those of $CeRu_2Si_2$ and UPt_3. This implies either a comparable or larger Zeeman energy in $CeIrIn_5$. Recently, the IEM in $CeIrIn_5$ was attributed to a valence transition[58] in which case we would also expect a change in the Fermi Surface volume. Our data appears to rule out this as a possibility. Thus, our data indicates that neither the Zeeman splitting, and associated proximity to a van Hove singularity, nor f-electron localization, or even valence fluctuations are the driving mechanisms for IEM in $CeIrIn_5$.

Despite the lack of drastic changes in neither the dHvA frequencies nor effective masses, we observe distinct changes in the dHvA signal near H_m. Namely, the metamagnetic transition is accompanied by an overall damping of the dHvA oscillations. This can be directly observed on the background subtracted torque signal of Fig. 5. At $\Theta = -1^\circ$ (Fig. 5a), only the lowest frequency α_3 oscillations are observed above the transition field $H_m = 27.5T$, the β_2 oscillations being completely suppressed in the field polarized state. At $\Theta = 29^\circ$ (Fig. 5b), where α_3 is the only frequency present in the entire field range, we see

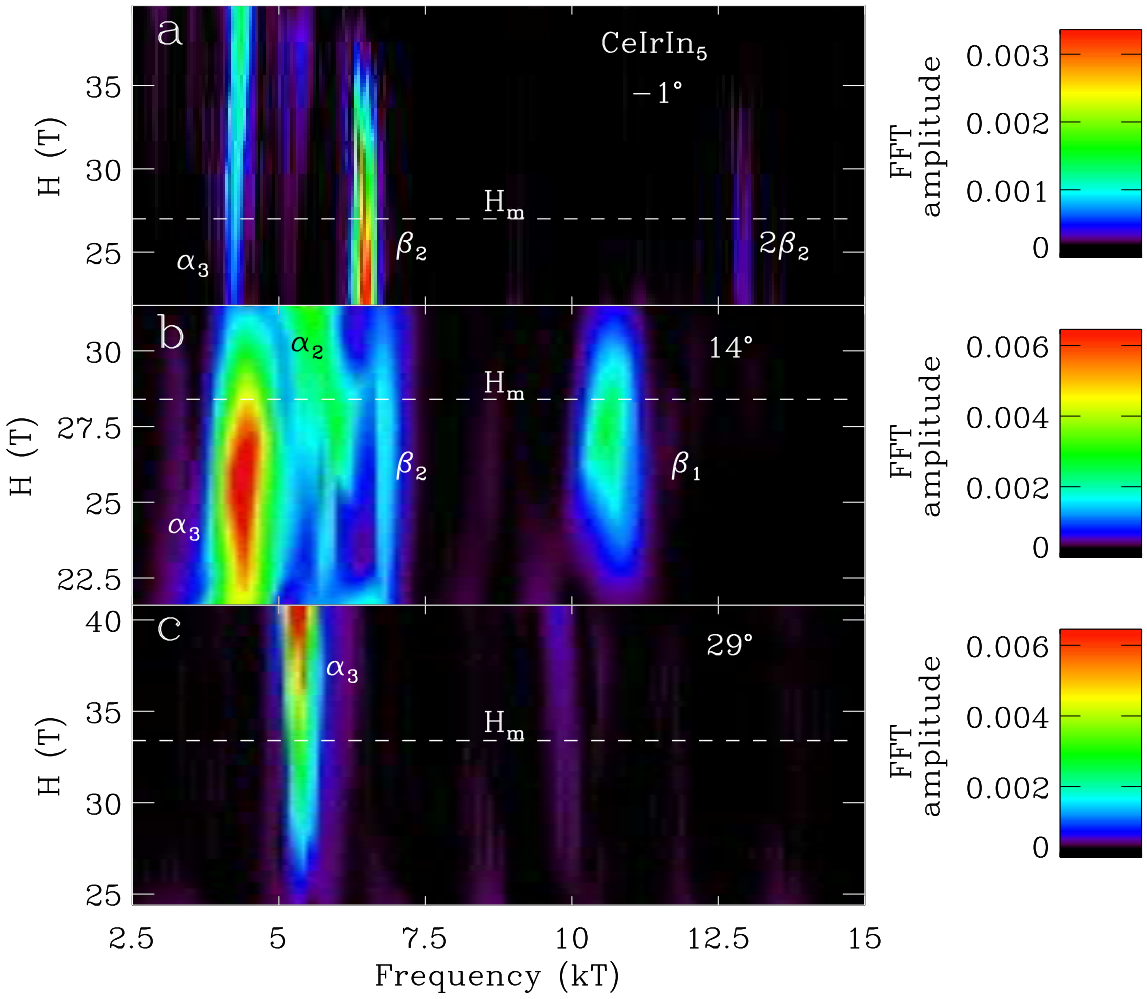

FIG. 8: de Haas-van Alphen amplitude variation near the metamagnetic critical field in $CeIrIn_5$. Contour plot of the FFT Amplitude vs. frequency and magnetic field, H, at $T = 40$ mK and (a) $\Theta = -1°$, (b) 14°, and (c) 29°. The FFT spectra was obtained on a field interval centered around the indicated fields, all intervals being of equal length in H^{-1}, the length chosen to correspond to 29 periods (panel a,c) and 23 periods (panel b) of α_3. The α_1 and α_2 orbits are not well resolved due to the smaller field range of the FFT leading to broader peaks. The high frequency peak in (a) is the second harmonic of the β_2 orbit.

clearly that the amplitude of the oscillations does not increase monotonically with magnetic field but instead goes through a minimum around $H_m = 33.4T$. The field evolution of the FFT spectra for three representative angles (−1°, 14° and 29°) is depicted on the contour plots of the dHvA amplitude vs magnetic field and frequency in Fig. 8. The frequencies of the α_3, β_1 and β_2 orbits being all field independent, the corresponding contours stretch

vertically. As clearly seen in Fig. 8, the amplitude of the β_2 orbit is completely suppressed at -1° in the field polarized state above H_m. A similar trend is also seen for the β_1 peaks at 14° (the data is only available up to 33 T at this angle). The β_2 peak at 14° is not easily distinguished from the neighboring α_1, α_2 peaks in the spectra due to the insufficient frequency resolution for small field ranges used in the FFT. In contrast, the amplitude of the α_3 peak is largest in the field polarized state after going through a minimum at a field just above H_m.

One can see this trend more clearly in the corresponding Dingle plots, shown for the same angles (-1°, 14° and 29°) as well as for several others in Fig. 9. Here the reduced dHvA amplitude as a function of inverse magnetic field H^{-1} is displayed. The reduced amplitude is defined as $\ln(A\frac{sinh(xT)}{xTH^{\frac{3}{2}}})$, where A is the FFT amplitude of each orbit. According to the LK theory (see Ref.[49], p.66), the reduced amplitude should be linear in inverse field. As seen in Fig. 9a, this is not the case in $CeIrIn_5$ and the amplitudes of the β_1 and β_2 oscillations are strongly suppressed in the field polarized state for $H > H_m = 29$ T at 14°. Moreover, the suppression of the β_2 oscillations is not restricted to a particular angle but is systematically observed for the entire range where this orbit is resolved ($-8^\circ \leq \Theta \leq +14^\circ$), as shown in Fig. 9b. In contrast, the amplitude of the α_3 oscillations go through a minimum above the transition but recover at higher fields, as shown in Fig. 9c for various angles ranging from -28° to $+29^\circ$. The maximum in the amplitudes of both α_3 and β_2 moves to higher fields (smaller H^{-1}) with increasing angle, following the same trend as H_m (see Figs. 9(b), 9(c)). Thus, the main result of our investigations is that there is a selective damping of the dHvA oscillations in the field-polarized state, due to the metamagnetic transition.

In LK theory, the slope of the Dingle plot corresponds to the Dingle temperature defined as $T_D = \frac{\hbar\tau^{-1}}{2\pi k_B}$, with τ^{-1} the scattering rate on each orbit describing the impurity broadening of the Landau levels at low-T[49]. For α_3 and β_2 orbits, Dingle temperatures of 0.31 and 0.27 K were obtained from linear fits to the reduced amplitudes in the low field state, for $\Theta = -8^\circ$, using the effective masses determined independently from the LK fits (see above). These correspond to a mean free path of 112 nm for the α_3 orbit and 172 nm for the β_2 orbit which compares well to the value of 105 nm reported previously[51]. The scattering rate associated with such values of ℓ is of the order of 3 THz, which is an order of magnitude less than the scattering time estimated from ρ_0. This is not surprising given the crude one band, one relaxation time approximation of the Drude formula as well as the differences

in the effective cyclotron masses and that estimated from the Sommerfeld model and γ_0 ($\sim 260m_e$) used in Eq. 1. Nevertheless, the fact that the Dingle temperatures for both orbits are $\sim$ 0.3 K which is of the order of both T_0 and T_{min} (see above) suggests that the transport is indeed in the diffusive regime with predominant disorder scattering. For β_1, we could not determine T_D since the Dingle plot is not linear in the inverse magnetic field, even in the low field state (see Fig. 9a). Thus the scattering rate for this orbit, as well as the effective mass (see above), appear to be somewhat field dependent, leading to a breakdown of the Dingle analysis.

The observed decrease in the amplitude of the dHvA oscillations above H_m for some of the observed branches is unexpected for at least two reasons. First, the spin fluctuations are suppressed in a field-polarized state which would indicate a smaller scattering rate, and thus larger oscillation amplitudes. Second, if one takes into account the magnetization in the dHvA effect, in fact the oscillations are in B^{-1} rather than in H^{-1}, one would also expect a positive feedback with the larger internal field giving rise to a larger amplitude of the oscillations. A reduction of the amplitude for all of the orbits near H_m may indicate an increased scattering rate due to electron scattering from magnetic fluctuations which are expected to be maximized at the phase transition.

There are several reasons for a decreased dHvA amplitude at high magnetic fields that are understood from extensive dHvA experiments in simple metals. One such possibility for a decreased dHvA amplitude is the so-called magnetic interaction leading to phase smearing[49], corresponding to the suppression of the overall signal due to electrons out-of-phase with one another in different parts of the sample. The underlying assumption is that the sample is either inhomogeneous in real space or that there is an inhomogeneous internal field distribution. In fact, if the magnetization is large then there will be an internal field inhomogeneity in the sample due to the shape dependent demagnetizing factor. Such an inhomogeneity would cause the dHvA amplitude to be smaller than when the field is homogeneous throughout the sample. This internal field correction is relevant when the magnetization of the sample is large. From the magnetization measured with a commercial SQUID at 1.8 K at an applied field of 7 T, we have extrapolated the volume magnetization in $CeIrIn_5$ to be about 326 G at 30 T (without taking into account the increase in M due

to the metamagnetic transition), which is 3 orders of magnitude smaller than the external field. Unless the sample itself is in an intrinsically inhomogeneous state, we are safe in assuming that $B \approx H$ is nearly homogeneous. To the best of our knowledge, no evidence for sample inhomogeneity is reported in the undoped, highly stoichiometric, high quality single crystals of $CeIrIn_5$. Also it is not clear how this effect would lead to preferential damping of the β orbits, nor to the damping only in the field polarized state. Thus phase smearing is unlikely to be the cause of the observed damping.

A second possibility for a non-linear Dingle plot is the magnetic breakdown for the β orbits. Magnetic breakdown happens when the applied field is strong enough that the electrons tunnel from one piece of the Fermi Surface to another, leading to the observation of large dHvA frequencies[49]. Since we do not see any new frequencies appearing in the field polarized state, this is unlikely in our case. Finally, the dHvA amplitude can be suppressed due to the spin reduction factor, namely the destructive interference between the Zeeman split up- and down-spin electrons. Although we cannot resolve this splitting in the dHvA frequencies, such a polarization would lead to a decrease of the dHvA amplitudes. The spin reduction factor[49], $R_s = cos(\frac{\pi g m*}{2m})$, can be estimated for various orbits using the cyclotron effective masses determined above and with a Lande factor $g = 2$, yielding the same reduction factor for α and β orbits. Thus we can rule out Zeeman splitting as the cause of selective damping of dHvA oscillations above H_m.

Thus, one is lead to conclude that there has to be an additional damping mechanism beyond those typically considered (thermal and disorder broadening or Zeeman splitting) in the LK theory. Perhaps the most noteworthy aspect of our data is that the damping is selective: the heavier $\beta-$orbits are more strongly damped than the lighter $\alpha-$orbits, being totally suppressed in the field-polarized state. Although the cyclotron mass of all observed orbits does not change appreciably across the transition, a lighter heavy fermion ground state in the high field state would result due to this selective suppression of heavy quasiparticles from the heavier β-sheet. It is also interesting to note that the β orbits are associated with the same hole band for which the smallest of the four hybridization gaps, namely Δ_1, has been assigned in optical conductivity measurements[33]. Although the interpretation of optical conductivity data may not be unique, it points to the same trend

in the evolution of this gap across the $CeMIn_5$ family as the systematic changes found in other characteristic parameters such as γ and T_c[33].

The decreasing dHvA amplitudes for the $\beta-$orbits above H_m are also difficult to reconcile with the simultaneous drop in ρ. Assuming that ρ is determined by parallel conduction channels associated with each Landau orbit, and since the heavier $\beta-$orbits (with smaller conductivity) are preferentially damped above H_m, this would lead to an increased ρ, making necessary a simultaneous enhancement of the mean free path ℓ of the light carriers in order to have a decreased ρ. Thus, the transport is most likely dominated by the lighter electrons on the α sheet that are strongly scattered near the transition but are otherwise intact in the field-polarized state. This is a possible explanation of the apparent paradox of a simultaneous decrease in both ρ and the dHvA amplitudes across the IEM transition.

V. CONCLUSION

In conclusion, our comparative study of ρ and dHvA oscillations is suggestive of an unusual metamagnetic transition in $CeIrIn_5$. The observed deviations from quadratic behavior in ρ vs T above as well as below H_m, may well correspond to a non-Fermi Liquid regime extending over a wide range of magnetic field in the phase diagram. In the field-polarized state, above 36 T, a Fermi liquid regime is recovered. Moreover, an upturn is observed in the $T-$dependence of ρ that is somewhat different from what is reported in $Sr_3Ru_2O_7$[20,21]. The $\rho(T)$ that we measure may correspond to quantum corrections that occur in a diffusively conducting strongly correlated metal. A detailed analysis of the dHvA oscillations shows that while the frequencies and effective masses are not significantly changed in the vicinity of the transition, the amplitude of some of the orbits are unexpectedly suppressed in the high field state. One possible way to reconcile the anomalous damping of the dHvA oscillations with the pronounced drop in the magnetoresistance is that the heavy holes are selectively damped across the IEM transition and that the transport is dominated by the lighter electrons. These results represent a challenge to our current understanding of IEM and call for further investigation as to what can cause such a change in the magnetization, the metamagnetic transition, beyond the mechanisms thus far explored, none of which can adequately account for the observed response in $CeIrIn_5$.

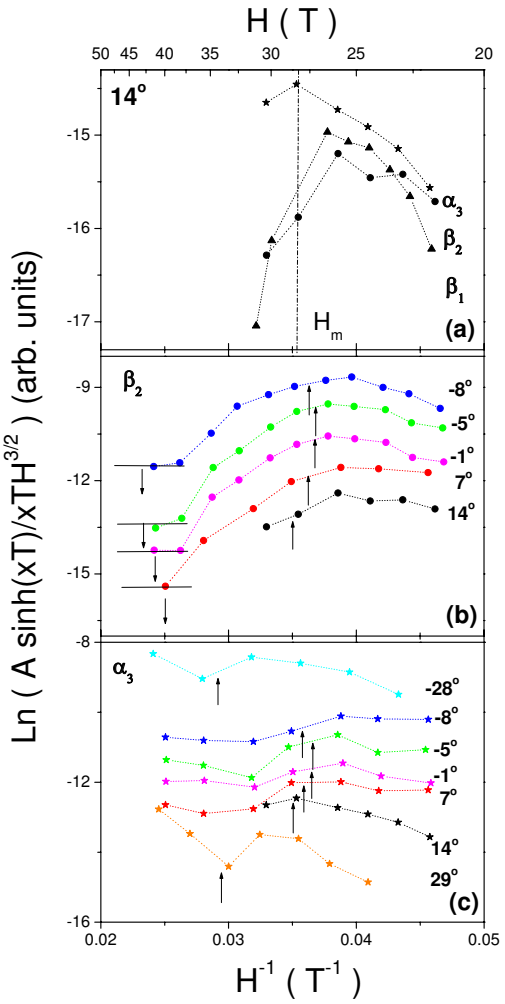

FIG. 9: Dingle Temperature analysis in $CeIrIn_5$. (a) Reduced amplitude $\ln(A\frac{sinh(xT)}{xTH^{\frac{3}{2}}})$ vs. inverse field H^{-1} for $\Theta = 14^o$ for the orbits α_3 ($\star$), β_1 ($\triangle$), β_2 ($\bullet$). For convenience, the corresponding field range is also indicated at the top of the figure. (b) Reduced amplitude vs inverse field for β_2 orbit at all angles where this frequency is resolved, angles ranging from $-8°$ to $14°$ as indicated. The horizontal lines with arrow correspond to the noise level of the FFT spectra giving an upper limit for the amplitudes at the highest fields. (c) Reduced amplitude vs inverse field for α_3 orbit at various angles. The data for all angles is up to 45 T, except for $\Theta = 14°$, which is limited to 33 T. The IEM transition field H_m is indicated for each angle with a vertical arrow.

Acknowledgments

We acknowledge fruitful discussions with B.Binz, I. Vekhter, F. Ronning, P. Adams, A. Chubukov, P. Schlottmann, C. Varma and D.Pines. Work at Los Alamos was performed

under the auspices of the U.S. Department of Energy. A portion of this work was performed at the National High Magnetic Field Laboratory, with support from the NSF Cooperative Agreement No. DMR-0084173, by the State of Florida, and by the DOE. Work at LSU was supported by NSF under grant no. DMR-0804376.

---

* Present affiliation: Physical Review Letters

[1] E. P. Wohlfarth, P. Rhodes, Philos. Mag. **7**, 1817 (1962).

[2] T. Goto, K. Fukamichi, H. Yamada, Physica B **300**, 167 (2001).

[3] T. D. Matsuda, H. Sugawara, Y. Aoki, H. Sato, A. V. Andreev, Y. Shiokawa, V. Sechovsky, L. Havela, Phys. Rev. B **62**, 13852 (2000).

[4] P. H. Frings, J. M. M. Franse, F. R. de Boer, A. Menovsky, J. Mag. Mag. Materials **31-34**, 240 (1983).

[5] J. Flouquet, P. Haen, S. Raymond, D. Aoki, G. Knebel, Physica B **319**, 251 (2002).

[6] H. Yamada, Phys. Rev. B **47**, 11211 (1993).

[7] H. Aoki, S. Uji, A. K. Albessard, Y. Onuki, Phys. Rev. Letters **71**, 2110 (1993).

[8] D. Meyer, W. Nolting, Phys. Rev. B **64**, 052402 (2001).

[9] H. Satoh, F. J. Ohkawa, Phys. Rev. B **57**, 5891 (1998).

[10] J. Rossat-Mignod, L. P. Regnault, J. L. Jacoud, C. Vettier, P. Lejay, J. Flouquet, E. Walker, D. Jaccard, A. Amato, J. Magn. Magn. Matter **76-77**, 376 (1988).

[11] N. Harrison, S. E. Sebastian, C. H. Mielke, A. Paris, M. J. Gordon, C. A. Swenson, D. G. Rickel, M. D. Pacheco, P. F. Ruminer, J. B. Schillig, J. R. Sims, A. H. Lacerda, M. T. Suzuki, H. Harima, T. Ebihara, Phys. Rev. Lett. **99**, 056401 (2007).

[12] P. M. C. Rourke, A. McCollam, G. Lapertot, G. Knebel, J. Flouquet, S. R. Julian, Phys. Rev. Lett. **101**, 237205 (2008).

[13] H. Shishido, R. Settai, H. Harima, Y. Onuki, J. Phys. Soc. Jpn. **74**, 1103 (2005).

[14] R. S. Perry, L. M. Galvin, S. A. Grigera, L. Capogna, A. J. Schofield, A. P. Mackenzie, M. Chiao, S. R. Julian, S. I. Ikeda, S. Nakatsuji, Y. Maeno, C. Pfleiderer, Phys. Rev. Lett. **86**, 2661 (2001).

[15] S. A. Grigera, R. S. Perry, A. J. Schofield, M. Chiao, S. R. Julian, G. G. Lonzarich, S. I. Ikeda, Y. Maeno, A. J. Millis, A. P. Mackenzie, Science **294**, 329 (2001).

[16] Z. Q. Mao, M. Zhou, J. Hooper, V. Golub, C. J. O'Connor, Phys. Rev. Lett. **96**, 077205 (2006).

[17] P. Gegenwart, F. Weickert, M. Garst, R. S. Perry, Y. Maeno,Phys. Rev. Lett. **96**, 136402 (2006).

[18] K. Kitagawa, K. Ishida, R. S. Perry, T. Tayama, T. Sakakibara, Y. Maeno, Phys. Rev. Lett. **95**, 127001 (2005).

[19] A. J. Millis, A. J. Schofield, G. G. Lonzarich, S. A. Grigera, Phys. Rev. Lett. **88**, 217204 (2002).

[20] R. S. Perry, K. Kitagawa, S. A. Grigera, R. A. Borzi, A. P. Mackenzie, K. Ishida, Y. Maeno, Phys. Rev. Lett. **92**, 166602 (2004).

[21] R. A. Borzi, S. A. Grigera, J. Farrell, R. S. Perry, S. J. S. Lister, S. L. Lee, D. A. Tennant, Y. Maeno, A. P. Mackenzie, Science **315**, 214 (2007).

[22] B. Binz, H. B. Braun, T. M. Rice, M. Sigrist, Phys. Rev. Lett. **96**, 196406 (2006).

[23] T. Takeuchi, T. Inoue, K. Sugiyama, D. Aoki, Y. Tokiwa, Y. Haga, K. Kindo, Y. Onuki, J. Phys. Soc. Jpn. **70**, 877 (2001).

[24] E. C. Palm, T. P. Murphy, D. Hall, S. W. Tozer, R. G. Goodrich, J. L. Sarrao, Physica B **329-333**, 587 (2003).

[25] J. S. Kim, J. Alwood, P. Kumar, G. R. Stewart, Phys. Rev. B **65**, 174520 (2002).

[26] C. Petrovic, R. Movshovich, M. Jaime, P. G. Pagliuso, M. F. Hundley, J. L. Sarrao, Z. Fisk, J. D. Thompson, Europhys. Lett. **53**, 354 (2001).

[27] G. R. Stewart, Rev. Mod. Phys. **73**, 797 (2001).

[28] J. Paglione, M. A. Tanatar, D. G. Hawthorn, E. Boaknin, R. W. Hill, F. Ronning, M. Sutherland, L. Taillefer, C. Petrovic, P. C. Canfield, Phys. Rev. Lett. **91**, 246405 (2003).

[29] A. Bianchi, R. Movshovich, I. Vekhter, P. G. Pagliuso, J. L. Sarrao, Phys. Rev. Lett. **91**, 257001 (2003).

[30] F. Ronning, C. Capan, A. Bianchi, R. Movshovich, A. Lacerda, M. F. Hundley, J. D. Thompson, P. G. Pagliuso, J. L. Sarrao, Phys. Rev. B **71**, 104528 (2005).

[31] T. Park, F. Ronning, H. Q. Yuan, M. B. Salomon, R. Movshovich, J. L. Sarrao, J. D. Thompson, Nature **440**, 65 (2006).

[32] S. Nakatsuji, D. Pines, Z. Fisk, Phys. Rev. Lett. **92**, 016401 (2004).

[33] K. S. Burch, S. V. Dordevic, F. P. Mena, A. B. Kuzmenko, D. van der Marel, J. L. Sarrao, J. R. Jeffries, E. D. Bauer, M. B. Maple, D. N. Basov, Phys. Rev. B **75**, 054523 (2007).

[34] J. H. Shim, K. Haule, G. Kotliar, Science **318**, 1615 (2007).

[35] C. Capan, A. Bianchi, F. Ronning, A. Lacerda, J. D. Thompson, M. F. Hundley, P. G. Pagliuso,

J. L. Sarrao, R. Movshovich, Phys. Rev. B **70**, 180502(R) (2004).

[36] C. Capan , R. G.Goodrich, J. F.DiTusa, L.Balicas, Y. J.Jo, T. P.Murphy, E. C.Palm, R.Movshovich, E. D.Bauer, M. F.Hundley, J. D.Thompson, J. L.Sarrao, D.Hall, S. W.Tozer, Physica B **403**, 797 (2008).

[37] R. Settai, H. Shishido, S. Ikeda, Y. Murakawa, M. Nakashima, D. Aoki, Y. Haga, H. Harima, Y. Onuki, J. Phys.: Condens. Matter **13**, L627 (2001).

[38] R. Hlubina , T. M.Rice, Phys. Rev. B. **51**, 9253 (1995).

[39] R. Daou, C. Bergemann, S. R. Julian, Phys. Rev. Lett. **96**, 026401 (2006).

[40] L. Taillefer , F.Piquemal, J. Flouquet ,Physica C **153-155**, 451 (1988).

[41] C. M. Varma, Phys. Rev. Lett. **79**, 1535 (1997).

[42] T. R. Kirkpatrick, D. Belitz, Phys. Rev. B. **53**, 14364 (1996)

[43] I. Paul, C. Pepin, B. N. Narozhny, D. L. Maslov, Phys. Rev. Lett. **95**, 017206 (2005).

[44] Y. B. Kim , A. J. Millis, Phys. Rev. B. **67**, 085102 (2003).

[45] N. Manyala, Nature **404**, 581 (2000).

[46] M. F. Hundley, A. Malinowski, P. G. Pagliuso, J. L. Sarrao, J. D. Thompson, Phys. Rev. B. **70**, 035113 (2004).

[47] S. Burdin, A. Georges, D. R. Grempel, Phys. Rev. Lett. **85**, 1048 (2000).

[48] L. Taillefer, R. Newbury, G. G. Lonzarich, Z. Fisk, J. L. Smith, J. Magn. Magn. Materials **63-64**, 372 (1987).

[49] D. Shoenberg, Magnetic Oscillations in Metals, Cambridge University Press (1984).

[50] H. Shishido, R. Settai, D. Aoki, S. Ikeda, H. Nakawaki, N. Nakamura, T. Iizuka, Y. Inada, K. Sugiyama, T. Takeuchi, K. Kindo, T. C. Kobayashi, Y. Haga, H. Harima, Y. Aoki, T. Namiki, H. Sato, Y. Onuki, J. Phys. Soc. Jpn **71**, 162 (2002).

[51] Y. Haga, Y. Inada, H. Harima, K. Oikawa, M. Murakawa, H. Nakawaki, Y. Tokiwa, D. Aoki, H. Shishido, S. Ikeda, N. Watanabe, Y. Onuki, Phys. Rev. B **63**, 060503(R) (2001).

[52] T. Ebihara, N. Harrison, M. Jaime, S. Uji, J. C. Lashley, Phys. Rev. Lett. **93**, 246401 (2004).

[53] D. Hall, L. Balicas, Z. Fisk, R. G. Goodrich, U. Alver, J. L. Sarrao, Phys. Rev. B **79**, 033106 (2009).

[54] H. Aoki, S. Uji, A. K. Albessard, Y. Onuki, Phys. Rev. Lett. **71**, 2110 (1993).

[55] M. Takashita, H. Aoki, T. Terashima, S. Uji, K. Maezawa, R. Settai, Y. Onuki, J. Phys. Soc. Jpn. **65**, 515 (1996).

[56] R. A. Borzi, S. A. Grigera, R. S. Perry, N. Kikugawa, K. Kitagawa, Y. Maeno, A. P. Mackenzie, Phys. Rev. Lett. **92**, 216403 (2004).

[57] S. R. Julian, P. A. A. Teunissen, S. A. J. Wiegers, Phys. Rev. B **46**, 9821 (1992).

[58] S. Watanabe, A. Tsuruta, K. Miyake, J. Flouquet, Phys. Rev. Lett. **100**, 236401 (2008).